SENCKENBERG
world of biodiversity

New mandibular remains of *Callistoe* (Metatheria, Sparassodonta) reveal unexpected anatomical, functional, and evolutionary aspects of this carnivorous genus

Festschrift in Honour of Professor Dr. Wolfgang Maier
Edited by Ingmar Werneburg & Irina Ruf

M. Judith Babot[1], Guillermo W. Rougier[2], Daniel A. García-López[3,4], Sara B. Bertelli[5], Claudia M. Herrera[3,4], M. Virginia Deraco[3,4], Norberto P. Giannini[3,5]

1 *CONICET–Fundación Miguel Lillo. Miguel Lillo 251, T4000JFE, Tucumán, Argentina*

2 *Department of Anatomical Sciences and Neurobiology, University of Louisville, 511 S. Floyd Street, Louisville, Kentucky, 40202, U.S.A.; grougier@louisville.edu*

3 *Facultad de Ciencias Naturales e Instituto Miguel Lillo-Universidad Nacional de Tucumán, Miguel Lillo 205, T4000JFE, Tucumán, Argentina*

4 *Instituto Superior de Correlación Geológica-CONICET-Universidad Nacional de Tucumán. Yerba Buena, Argentina; dgarcialopez@csnat.unt.edu.ar, claucordoba@hotmail.com, virginiaderaco@gmail.com*

5 *Unidad Ejecutora Lillo–CONICET–Fundación Miguel Lillo, Miguel Lillo 251, T4000JFE, Tucumán, Argentina; sbertelli@lillo.org.ar, norberto.giannini@gmail.com*

http://zoobank.org/FE58A009-D441-4E56-A16B-482B08951947

Corresponding author: M. Judith Babot (mjbabot@lillo.org.ar)

Citation: Babot MJ, Rougier GW, García-López DA, Bertelli SB, Herrera CM, Deraco MV, Giannini NP (2022) New mandibular remains of *Callistoe* (Metatheria, Sparassodonta) reveal unexpected anatomical, functional, and evolutionary aspects of this carnivorous genus. Vertebrate Zoology 72 469–485. https://doi.org/10.3897/vz.72.e82709

Abstract

We present a detailed description of the anatomy of the dentary and lower teeth of a new specimen of *Callistoe vincei*, a large carnivorous metatherian from the Eocene (?Ypresian) of northwestern Argentina. The recently collected specimen is a young adult represented by a partial right dentary with the canine, p1, roots of p3, and very well-preserved m1 to m4. The description includes a comparison with the holotype specimen, a much older individual, and other closely related large sparassodonts (e.g., *Arminiheringia*). The analysis of this new material allowed identifying plesiomorphic molar features in *Callistoe*, such as the presence of a reduced metaconid on the m3 and a tricuspated, basined talonid on m1–m3. We also described the mesowear facets in the lower dentition, showing that the self-sharpening facet typically present in extinct and extant placental and some marsupial carnivorous forms, was absent in *Callistoe*. The presence of a short-term cutting edge in the trigonid related to the thinness of the enamel layer, and the associated tooth wear susceptibility, were likely compensated by a dental mechanism (overeruption) to maintain occlusal contact among antagonist teeth. This process could explain the marked extrusion of the tooth roots observed in *Callistoe* as well as in other large closely related members of the group.

Keywords

Callistoe vincei, carnivory, Eocene, Lumbrera Formation, South America, wear facets

Introduction

Callistoe vincei is a large metatherian recorded in northwestern Argentina during the ?early Eocene (Babot et al. 2002; Babot 2005; Argot and Babot 2011). It is one of the best preserved Paleogene species of Sparassodonta, the clade forming the bulk of the mammalian carnivorous guild during most of the Cenozoic in South America (Ameghino 1887; Simpson 1948, 1971; Marshall 1978; Forasiepi 2009; Forasiepi et al. 2015; Prevosti and Forasiepi 2018). Sparassodonta is widely regarded as monophyletic, although the inclusion of early Paleocene small metatherians from Bolivia in the group (*Mayulestes*, *Allqokirus*, *Pucadelphys*, and *Andinodelphys*) is still under debate (Marshall et al. 1990; Rougier et al. 1998; Forasiepi et al. 2015; Muizon et al. 1997, 2018; Muizon 1998; Engelman et al. 2020; Muizon and Ladevèze 2020).

Currently, *Callistoe vincei* is known only from the type (PVL 4187) and two very fragmented specimens (PVL 4207 and MLP 88-V-10-4). This hypercarnivorous sparassodont is characterized by an elongated skull, nasal anteriorly extended, conspicuous postorbital process, glenoid process of the jugal well developed, tympanic process of the alisphenoid absent, exit of the mandibular branch of the trigeminal (V3) identified as a simple aperture limited by the alisphenoid and the petrosal, mandibular symphysis fused and extended to the limit between the p3 and m1, ventral border of the dentary convex, dental formula I4/i3, C/c, P3/p3, M4/m4, upper and lower canines with opened roots in adult forms (but probably closed at later ontogenetic stages), upper and lower third premolar with enlarged roots and lateromedially compressed not bulbous crown, paracone and lingual side of the upper molars —including protocone— reduced, and U-shaped long postmetacrista. Among lower molars, only the morphology of the m4 was known up to date: the protoconid is the main cuspid, while the metaconid is absent, and the very reduced talonid only bears one cusp, initially interpreted as a hypoconulid (Babot et al. 2002; Babot 2005).

Callistoe was a large sparassodont, with a body mass calculated between ∼ 20 kg and ∼ 34 kg (Babot 2005; Argot and Babot 2011; Prevosti et al. 2013; Croft et al. 2018). The dentition, the skull, and mandibular shape clearly indicate hypercanivory (Babot 2005; Blanco et al. 2011; Prevosti et al. 2013; Echarri et al. 2017), and the postcranial skeleton suggests terrestrial habits, with likely fossorial capabilities (Babot 2005; Argot and Babot 2011).

Traditionally, *Callistoe* has been grouped in the Family Proborhyaenidae together with *Arminiheringia*, *Paraborhyaena*, and *Proborhyaena*, although the monophyly of the family has been questioned (Babot et al. 2002). In a broader phylogenetic context, *Callistoe* is recovered as a nested member of Borhyaenoidea, and as the sister taxon of alternatively *Arminiheringia* (Babot 2005), *Paraborhyaena* (Babot et al. 2002; Engelman and Croft 2014; Forasiepi et al. 2015; Muizon and Ladevèze 2020), or as a basal Proborhyaenidae (Engelman et al. 2018, 2020).

Here, we consider *Callistoe vincei* as a distal Borhyaenoidea, and sister taxon of *Arminiheringia auceta*, based on the fact that these genera share the following synapomorphies: canines with very thin enamel layer which is lost in advanced wear stages, and presence of a sulcus in the posterolateral border of the palatine related with the transmission of vessels from the minor palatine foramen to the soft palate (Babot 2005). The relationships between *Callistoe* with other traditionally considered proborhyaenids (*Proborhyaena*, *Paraborhyaena*) cannot be established until the discovery of better preserved specimens of these genera.

We describe here the anatomy and mesowear facets of a new specimen of *Callistoe vincei* collected from Lower Lumbrera Formation exposed at Pampa Grande, Salta Province (NW Argentina) and compare it with the type specimen (PVL 4187) and other closely related members of Sparassodonta —e.g., *Arminiheringia*. The age of these Eocene deposits, traditionally considered middle Eocene (Casamayoran SALMA; Pascual et al. 1981; del Papa et al. 2010; Powell et al. 2011) is now interpreted as probably early Eocene (Itaboraian SALMA, ?Ypresian; del Papa et al. 2022; see also Fernicola et al. 2021). The new material of *Callistoe* consists of a right fragment of mandible with canine, p1, and m1 to m4. The dentition is very well preserved, showing unexpected lower molar morphology that allows a more complete interpretation of the lower molar evolution in Sparassodonta.

Institutional abbreviations

AMNH American Museum of Natural History, New York, USA; **IBIGEO-P** Instituto de Biología y Geología, Colección de Paleontología, Salta, Argentina; **MACN-A** Museo Argentino de Ciencias Naturales "Bernardino Rivadavia", Colección Ameghino; Buenos Aires, Argentina; **MACN-PV** Museo Argentino de Ciencias Naturales "Bernardino Rivadavia", Colección Paleontología de Vertebrados; **MLP** Museo de La Plata, La Plata, Argentina; **MNHN-DP** Museo Nacional de Historia Natural, Montevideo, Uruguay; **PVL** Paleontología de Vertebrados Lillo, Tucumán, Argentina.

Anatomical abbreviations

m1–m4 first to fourth lower molars; **CEJ** cementumenamel junction.

A

B
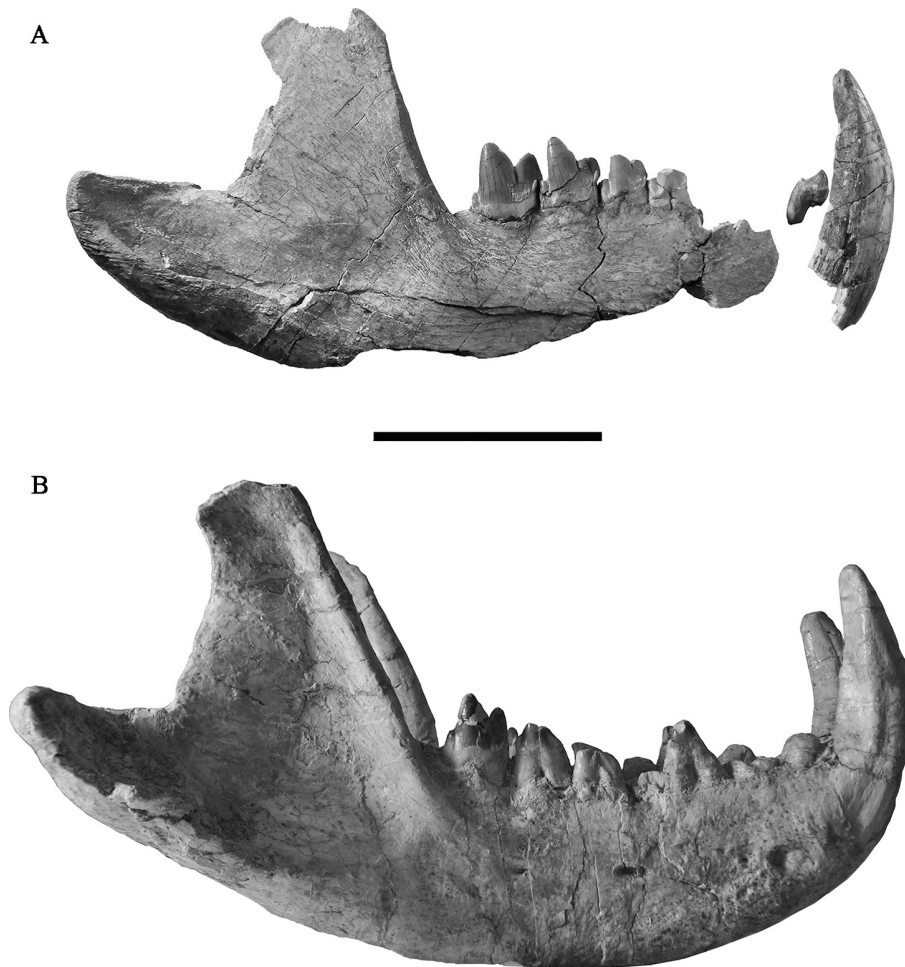
Figure 1. Mandible of *Callistoe vincei*. **A** IBIGEO-P 110, right dentary partially preserved, in lateral view. The position of the isolated canine and p1 was inferred from the proportion in the holotype; **B** complete dentary of the type specimen (PVL 4187). Scale bar: 5 cm.

Results

Systematic paleontology

Mammalia Linnaeus, 1758
Metatheria Huxley, 1880
Sparassodonta Ameghino, 1894
Callistoe **Babot, Powell, and Muizon, 2002**
Callistoe vincei **Babot, Powell, and Muizon, 2002**

Referred material. IBIGEO-P 110, fragment of right mandible with partial intra alveolar and complete extra alveolar portion of the canine, p1 with complete crown and distal root, roots of the p3, and complete m1 to m4 (Fig. 1A).

Locality and stratigraphic range. Pampa Grande, Guachipas Department, Salta Province, Argentina (25°46.95'S; 65°26.57'W). Lower Lumbrera Formation (?Ypresian; del Papa et al. 2022; see also Fernicola et al. 2021).

Description

The fossil preserves the distal two-thirds of the right jaw including the condyle, the coronoid process and the full molar series, in addition to an isolated right canine and p1 (Figs 1, 2A–C). This material represents a smaller specimen than the holotype (see molar and mandibular sizes; Tables 1, 2; Fig. 1), probably a young-adult individual, judging from the incomplete development of the coronoid process and the presence of a recently erupted (unworn) m4. Following the individual dental age stages (IDAS) proposed by Anders et al. (2011), this specimen falls into IDAS 3 category, which is defined by the presence of fully erupted dentition with wear restricted to the inner occlusal surface —absence of interior enamel and persistence of the external enamel border— on the m1. In the particular case of this specimen, only the m1 has lost by wear the paraconid and protoconid, remaining in the molar the truncated bases of these cuspids, with the enamel confined to the periphery; on the talonid of this tooth, the wear is restricted to the hypoconid apex.

Dentary. The dentary preserves part of the body —the upper half of the alveolar process bearing the p3 roots and the m1 to m4— and the almost complete ramus, except for the anterior part of the ventral border and the angular process (Figs 1, 2A–C). The lateral side of the body shows the posterior portion of the rim of a mental foramen located between the m1 and m2. In the holotype, the size and position of the mental foramina varies in each hemimandible. The foramen present in the specimen IBIGEO-P 110, is in the same position as the third mental foramen on the right body of the holotype (Fig. 1B). Bellow the boundary between the m3 and m4, the
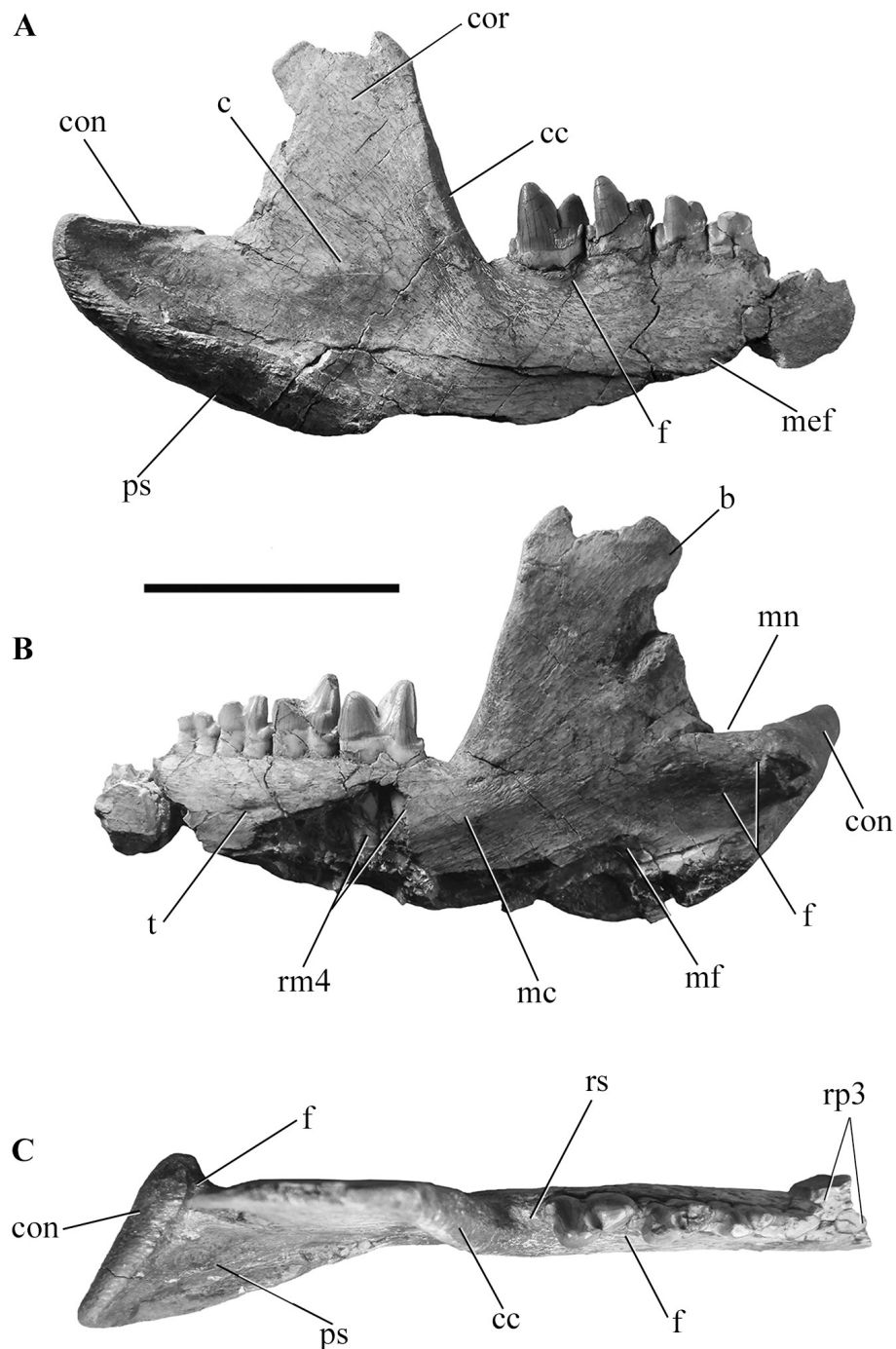
Figure 2. *Callistoe vincei* IBIGEO-P 110. Right dentary partially preserved in **A** lateral; **B** medial; and **C** dorsal views. Abbreviations: **b** beak; **c** crest; **cc** coronoid crest; **con** condylar process; **cor** coronoid process; **f** fossa; **mc** mylohyoid crest; **mf** mandibular foramen; **mef** mental foramen; **mn** mandibular notch; **ps** posterior shelf of the masseteric fossa; **rm4** roots of the m4; **rp3** roots of the p3; **rs** retromolar space; **t** tuberosities. Scale bar: 5 cm.

lateral aspect of the body presents a deep fossa, which is also present in the type specimen (PVL 4187), particularly emphasized on the left dentary. This pit, together with a shallow fossa extended anteriorly toward the alveolar border of the m1, could be related with the attachment of the buccinator muscle (following the pattern described in *Didelphis*; Hiiemae and Jenkins 1969). Behind the m4, the retromolar space is short, in agreement with the age stage inferred for this specimen. The medial side of the mandible is more fragmented (Fig. 2B) because part of the covering bone was lost, exposing the large roots of the last molar deeply implanted in the dentary. Medial to the roots of the p3, the mandibular bone expands medially, suggesting the location of the posterior extension of the symphysis which in the holotype reaches the point below the p3 and m1 limit. Below the m2 and m3 there are subtle tuberosities, also present in the holotype where they are located more anteriorly, below the m1 and m2. These structures could be related with the attachment of the geniohyoideus and genioglossus muscles, although in *Didelphis* it occupies a more ventral position (Hiiemae and Jenkins 1969, fig. 4B).

Table 1. *Callistoe vincei*. Measurements (in mm) of the dentary of the specimens PVL 4187 (holotype) and IBIGEO-P 110. *Measure taken from the posterior end of the retromolar space to the anterior extreme of the mandibular notch.

Measurement	PVL 4187 (holotype)	IBIGEO-P 110
Total length	205.0	—
Maximum width at the symphyseal region	34.0	—
Length of the body (right)	122.6	—
Length of the ramus (right)	86.9	62.7
Length of the coronoid process* (right)	58.6	46.5
Height of the mandibular body below m1 (labial and left)	43.0	—
Height of the mandibular body below m4 (labial and left)	47.5	—
Height of the posterior border of the coronoid process (right)	45.3	33.0
Width of the condyloid process (right)	35.5	32.5
Maximum width between right and left condyloid processes	122.0	—

Table 2. *Callistoe vincei*. Measurements (in mm) of the lower dentitions of the specimens PVL 4187 (holotype) and IBIGEO-P 110. **L** length; **W** width; **max** maximum length and width. Measurements were taken at the level of the alveolar border, except those with (*) that were taken at the crown level.

Dental locus		PVL 4187 (holotype)	IBIGEO-P 110
c (max)	L	18.6	15.6
	W	12.7	9.5
p1-m4	L	93.5	—
p1	L	10.3	7.2*
	W	6.0	4.6
p2	L	13.5	—
	W	—	—
p3	L	8.5*	—
	W	4.5*	—
m1-m4	L	56.6	45.6
m1	L	—	8.0*
	W	—	4.5*
m2	L	13.5	10.7*
	W	7.0	5.5*
m3	L	15.0	13.4*
	W	7.3	7.6*
m4	L	17.0*	15.5*
	W	11.6*	9.0*

The ramus conserves the condylar process complete while the coronoid process is partially preserved. The coronoid process, shorter and lower than in the holotype, shows a thick and straight coronoid crest that forms an obtuse angle with the main axis of the dentary (Figs 1, 2). This crest extends anteriorly and basally up to the level of the m3–m4 limit. The dorsal border of the coronoid process appears to be rounded and ends in a posterior beak, also present in the holotype and several other sparassodonts (e.g., *Arctodictis*, *Cladosictis*). The posterior border of the coronoid process is anteriorly slanted and together with the coronoid crest determine a triangular-shaped coronoid process. In lateral view, the coronoid process is smooth, except for a subtle crest and fossa that could correspond to the attachment of the ventral extension of the M. zygomaticomandibularis. The prominent posterior shelf of the masseteric fossa, the area of attachment of the

superficial and deep masseter muscles (Turnbull 1970), is narrower than in the holotype.

In medial view (Fig. 2B), the mandibular ramus shows the medial wall of the mandibular foramen, located approximately in line with the tallest point of the coronoid process. Dorsal and anterior to the mandibular foramen, the dentary shows a horizontal crest. In the holotype, this mandibular area is better preserved and shows a more subtle crest extending from the m2 to the posterior end of the m4 –not as posterior as in IBIGEO-P 110. We interpret this structure as part of the mylohyoid line for the attachment of the M. mylohyoideus, following its similar location in the dog (Evans and de Lahunta 2013; fig. 6–22). Dorsoposterior to the mandibular foramen, the ramus bears a rounded fossa, apparently absent in the type specimen where the area is partially damaged. In IBIGEO-P 110 this depression occupies a similar position to that described by Ercoli et al. (2017; fig. 2D) in the Carnivora *Galictis cuja* where the lateral pterygoid muscle inserts in a position anterior and medial to the neck of the condylar process. Moreover, both the holotype and IBIGEO-P 110 exhibit a small pit just anterior to the articular head of the condylar process which is in agreement with the location of the pterygoid fovea in *Didelphis* (the insertion of the inferior head of the lateral pterygoid muscle; Hiiemae and Jenkins 1969; Diogo et al. 2016). For *Callistoe*, we interpret this pit and the fossa posterior to the mandibular foramen as possible areas related with the lateral pterygoid muscle attachment.

The condylar process is a bar located at the same level as the alveolar dorsal border. Due to postmortem deformation, it is not transverse to the main axis of the dentary, as expected anatomically, but orientated posterolaterally (Fig. 2C). The articular head narrows laterally and occupies the dorsal and posterior aspect of the process. The posterior side of the neck shows a deep fossa opened medially which would be related with the attachment of the lateral ligament, the fibrous part of the temporomandibular joint (Evans and de Lahunta 2013). The mandibular notch is open posteriorly and with a straight ventral side as in the holotype, but it is proportionately shorter, forming an almost right angle with the posterior border of the coronoid process.
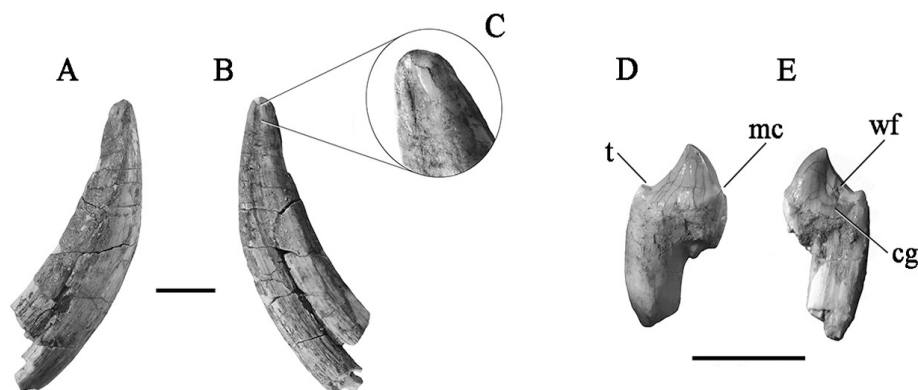
Figure 3. *Callistoe vincei* IBIGEO-P 110, right canine and p1. **A**, **B** canine in labial and lingual views, respectively; **C** detail of the canine tip in **B** showing the remnant enamel layer; **D** p1 in labial view; **E** p1 in lingual view. Abbreviations: **cg** cingulid; **mc** mesial cuspulid; **t** talonid; **wf** wear facet. Scale bar: 10 mm

Dentition. In addition to the complete teeth recovered in the dentary (m1 to m4), the dentition includes detached canine and p1, and roots of the p3 implanted in the alveoli. The teeth size in this specimen is about 20% smaller than the holotype (Table 2), which may be due to intraspecific variability or sexual dimorphism. Considering that the molar series in the new specimen measures 80% of that of the holotype, the assignment of the isolated premolar to the p1 is based on this same length proportion in relation to the p1 in the holotype. As mentioned, the teeth are only slightly worn, being the m1 the most affected tooth (see below).

The canine fragment mostly represents the extralveolar portion of the tooth (Fig. 3 A–C). It is large, pointed, and labiolingually compressed. The tooth is formed by dentine and enamel; the latter is preserved as a thin and very small sheet exposed on the lingual apex of the crown (Fig. 3C). This contradicts the initial assumption that the canine in *Callistoe vincei* lacked enamel (Babot et al. 2002); instead, it seems that the enamel is restricted to the most apical end of the tooth forming an enamel cap that wears down quickly. The canine exhibits a main wear surface which is present on the distolabial side and caused by the attrition with the lingual side of the upper canine. This facet is long, slightly concave, and well demarcated by distal and labial sharp borders. Several longitudinal striae, sulci, and grooves extend along the entire length of the canine, mainly on the lingual and distal sides. The deepest is the medial groove, followed by two shallower distal sulci. The remaining grooves are represented by striae close to each other, more marked towards the root of the tooth. The presence of a deep lingual sulcus is a common feature in Sparassodonta, emphasized in the larger members of the group (e.g., *Borhyaena*, *Australohyaena*; *Arminiheringia*, *Proborhyaena*; *Paraborhyaena*; Babot et al. 2002; Engelman et al. 2020).

The first premolar is almost complete, except for the mesial root, the most mesiobasal border of the crown, and the tip of the distal cuspid (Fig. 3D, E). The crown is asymmetric —the mesial border is convex and short and the distal one is concave and longer— and more convex on the labial half. The medial side is flatter than the lingual one. The mesial portion exhibits a small and labially located cuspulid from which arises a crest towards the apex of the protoconid. Lingual to the mesial cuspulid, but unconnected, there is a mesial cingulid broken for the most part. The distal portion of the p1 bears a partially preserved talonid probably supporting a small cuspid. The lingual side of the talonid exhibits a wear surface that partially removed a subtle cingulid.

The third premolar was lost before collection and is only represented by its roots. In the specimen IBIGEO-P 110 this tooth must have been completely erupted given that in Sparassodonta the third premolar erupts about the same time as the fourth molar (Forasiepi and Sánchez-Villagra 2014). The roots are rounded, subequal in diameter, and separated by a relative wide septum. In the holotype the p3 roots are very large —wider and longer than in the m1— and are greatly exposed over the alveolar border, aligning the apex of tooth crown almost at the same height as the apical portion of the m4.

In this specimen the molar row is complete and very well preserved, which is key because previously known specimen of *C. vincei*, preserve only one complete molar, the m4 (Figs 1B, 4A, B). The overall tooth size and the trigonid increase rapidly in size from the m1 to the m4 (Table 2). Some other traits of the trigonid, like the sharpness of the mesial keel and the deepness of the hypoconulid notch, also become more pronounced toward the posterior end of the molar row. The angle formed between the paracristid and the long axis of the dentary also increased posteriorly, because the protoconid is progressively set more labially. The length of the precingulid however, becomes shorter posteriorly. The talonid decreases in height and size from the m1 to m4 and the hypoflexid becomes deeper in the same direction. From the m1 to m3 the talonid conserves the same tricuspid pattern, but in the m4 the basin is greatly reduced and the cuspid arrangement is highly modified (see below). The basal extension of the molar enamel defines two lobes above the mesial and distal roots. From the m1 to the m3, the mesial lobe is more dorsally located than the distal lobe. In the m4, the enamel basal line is approximately straight, clearly visible in the type specimen. The molar roots protrude from the alveolar margin, —but in lesser extent than in the type specimen. In PVL 4187 the ex-
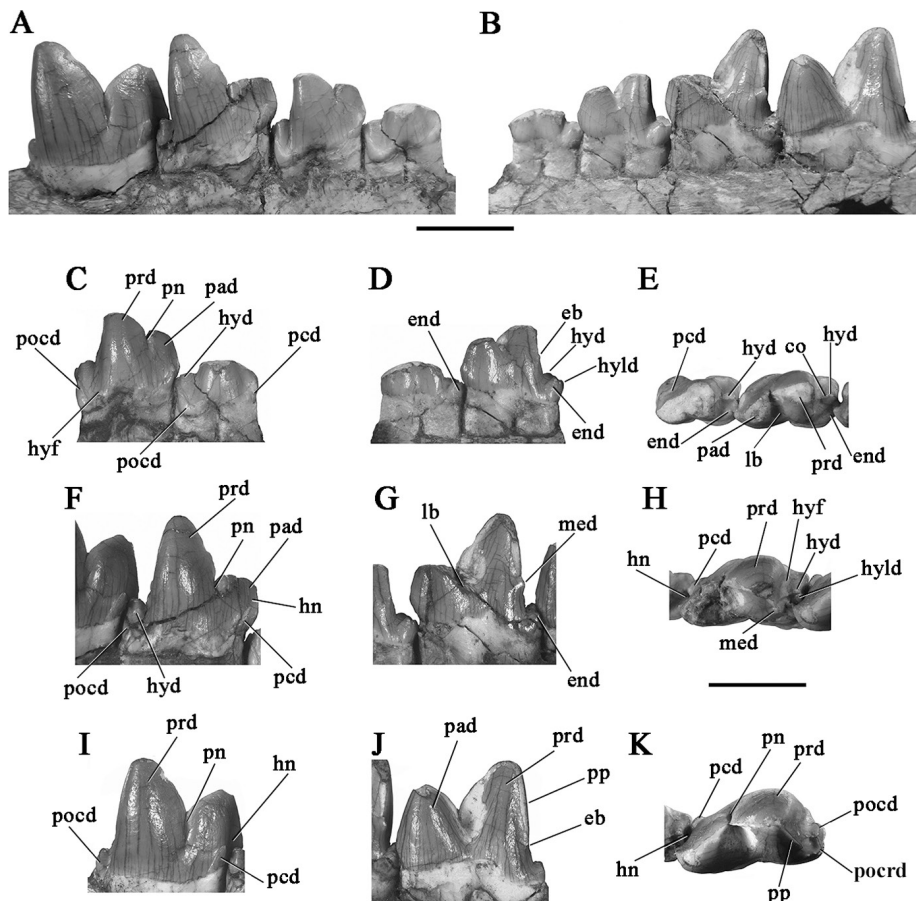
Figure 4. *Callistoe vincei* IBIGEO-P 110, right lower molar row. **A** labial view; **B** lingual view; **C** m1 and m2, labial view; **D** m1 and m2, lingual view; **E** m1 and m2, occlusal view; **F** m3, labial view; **G** m3, lingual view; **H** m3, occlusal view; **I** m4, labial view; **J** m4, lingual view; **K** m4, occlusal view. Abbreviations: **co** cristid obliqua; **eb** enamel bulge; **end** entoconid; **hn** hypoconulid notch; **hyd** hypoconid; **hyld** hypoconulid; **hyf** hypoflexid; **lb** lingual basin; **med** metaconid; **pad** paraconid; **pcd** precingulid; **pn** paracristid notch; **pocd** labial postcingulid; **pocrd** postcristid; **pp** postprotocristid; **prd** protoconid. Scale bar: 10 mm.

posed root surface in the m3 and m4 is larger than in IBIGEO-P 110.

On the m1 the trigonid does not preserve individual cusps, the paraconid and protoconid have been obliterated by wear against the distal side of the P3 (Fig. 4C–E). The exposed surface of the cusp bases indicates that the protoconid was the largest of the two. It was located labially to the paraconid, so that the paracristid was oblique, unlike the condition in e.g., *Pharsophorus* and *Australohyaena*, where this crest is straight and the paraconid, protoconid and hypoconid are in line with the mesiodistal axis of the tooth. The metaconid, which is present on the m3, could have been also present in the m1. This inference derives from a wear facet located on the mesiolingual corner of the trigonid; but given the absence of a metaconid in the m2, it is possible but unlikely. On the trigonid, the mesial border is not preserved and the presence of the hypoconulid notch cannot be described. The precingulid arises from a tiny cuspulid located slightly distolabial to the most mesial border of the tooth; it is partially worn and its most distal end diverges into two short dorsal and basal cingulids. The talonid is complete. It bears very well-preserved hypoconid, hypoconulid, and entoconid. The talonid width is nearly equal to the paraconid base but narrower than the

protoconid. The largest cusp is the hypoconid which is mesiodistally elongated and exhibits apical wear. From this cuspid a very short cristid obliqua reaches the distal wall of the protoconid in a middle position from where this notched crest runs upward, climbing the distal slope of the protoconid. The cristid obliqua is not as lingually directed as in the m2 and m3, defining a shallower hypoflexid than in the posterior molars. Distal and basal to the hypoconid, the talonid is surrounded by a labial postcingulid reaching the base of the protoconid where it limits a very narrow shelf. The hypoconulid is the lowest cuspid; it is labiolingually elongated, and occupies a distal and median position. The entoconid is conical, connected to the hypoconulid by a short postcristid which bears a tiny postentoconulid; the entoconid is disconnected from the protoconid, i.e., the entocristid is absent. The basin is shallow with a talonid notch broadly open lingually, reaching down the CEJ.

On the m2 the trigonid/talonid length ratio is higher than on the m1; i.e., the trigonid is larger than on the m1 but the talonid is only slightly larger (Fig. 4C–E). Therefore, the overall increase in length on the m2 is accomplish almost solely by the larger trigonid. Moreover, the acute angle formed by the paracristid and the mesiodistal axis of the tooth is also greater; i.e., the protoconid is

more labially located. The mesial portion of the trigonid exhibits a deep hypoconulid notch which separates the mesial border of the paraconid from the precingulid. This cingulid, which surrounds the labial aspect of the paraconid base almost until the paracristid notch, is broader near the hypoconulid notch; it weakens towards the base of the paraconid along its mesiolabial face where it ends in two tiny cuspulids. The paracristid notch (carnassial notch) is visible here although not as well developed as in the posterior molars. The protoconid is a triangular cusp with a flat distal face and a complex lingual morphology. As in other mammalian sectorial teeth, the lingual aspect of the protoconid is reinforced by a blunt ridge extending from the labial apex of the cusp, descending abruptly to reach the lingual margin of the crown. This crest divides the trigonid into two areas: a mesial concave surface and a less excavated distal surface. The mesial area is functionally part of the paracristid notch determining a broad and distinctive basin lingual to it. The distal surface produces a concave area running parallel to the postprotocristid that is much less developed than the mesial one. The sharpness of the paracristid and relative bluntness of the postprotocristid are determined to a large degree by the development of these features of the lingual aspect of the protoconid. The postprotocristid exhibits an enamel bulge in the same position as the metaconid in the m3. But considering the absence of a postprotocristid notch, we conclude that this bulge is not a true metaconid, just the undifferentiated portion of the crown not under the influence of a putative metaconid enamel knot. The talonid on the m2 is similar to that of the m1 in the general size and in the position and size of the cuspids. However, some structures are better preserved. The cristid obliqua forms a distinct notch when it reaches the protoconid; from this point the crest rises upward on the flat distal face of this cusp. Another notch is visible between the hypoconid and the hypoconulid, which are close together. The labial postcingulid is similar in shape and size to that of the m1. Between the hypoconulid and the entoconid, appears to be an elongated postentoconulid and a notch between both structures. The entoconid is a pointed cusp disconnected from the protoconid. Towards the base, it exhibits a minute cuspulid. The talonid basin is shallow and opens lingually in a well-demarcated talonid notch.

The third molar is larger than the mesial teeth (Fig. 4F–H; Table 2). This difference is due only to a trigonid increase in size; the talonid is smaller than in the m2, both in absolute terms and in relation to the trigonid. The hypoconulid notch is conspicuous. Towards the base it bears a short cingulid disjointed from the precingulid. The precingulid has a main short and crested segment, with two tiny cuspulids. The distal part is a weak shelf running to a point basal to the paracristid notch. As in the precedent teeth, the distal face of the protoconid is flat. The postprotocristid is sharp; it ends in a notch formed at the junction with a small and conical metaconid located in a somewhat basal position, below the level of the paraconid apex. The talonid is appressed against the m4; the three main cuspids are well-preserved, being the

hypoconid and the hypoconulid slightly larger than the entoconid. Unlike the condition of the m2, in the m3 all three talonid cusps are cone-shaped and appressed to each other. The cristid obliqua runs lingually to the protoconid, in a similar position to that of the precedent molars. This crest climbs the distal wall of the protoconid, next to the basal level of the metaconid. The talonid basin is small and it is virtually closed by the entoconid, although this cuspid does not reach completely the distal wall of the protoconid. The hypoconulid is distally located, in a central position of the distal talonid border. The labial postcingulid originates at the base of the hypoconulid; it surrounds the talonid towards the base of the hypoflexid, where this cingulid bears two tiny cuspulids.

The m4 is the largest and best preserved tooth (Figs 4I–K, 5). The roots are exposed on the medial side of the dentary, showing the depth of tooth insertion in the mandibular bone (Fig. 2B); the roots measure more than the half of the tooth crown (27 mm vs. 13 mm, respectively). The paracristid notch is a deep V-shaped efficient capturing structure where forces concentrate at the end of the stroke (Evans 2005). The hypoconulid notch is deeper than in the precedent molars; it lodges the hypoconulid and the entoconid of the m3. On the base, it bears a short cingulum which does not reach the precingulid, which is smaller and shorter than in the m3. The postprotocristid ends toward the base of the protoconid, but contrary to that observed on the m3, the protocristid notch and the metaconid are absent. The talonid is more reduced and modified in relation to the precedent molars and it has a variable morphology among the known specimens of *Callistoe* (Figs 4, 5). In the new specimen here described, we observe two evident cuspids on the talonid: the hypoconid and a labial accessory cuspid. The hypoconid is tiny and very close to the protoconid. The cristid obliqua is absent, given the proximity of the hypoconid with the protoconid, but its vertical extension at the distal face of the protoconid is present, as in the anterior molars. The labial accessory cuspid is linked, via a very short cristid, with the distal border of the talonid; from this point of contact, the labial postcingulid arises and runs mesially towards the hypoflexid. The hypoconulid is absent. The lingual side of the talonid is surrounded by the postcristid which ends in a tiny cuspule located at the base of the protoconid. Slightly distal, the postcristid exhibits an enamel bump that could represent a rudimentary entoconid, but this feature is so subtle as to lack any functional significance and we prefer to regard the entoconid as absent. In the holotype the talonid exhibits the hypoconid and the labial accessory cuspid. As in the specimen IBIGEO-P 110 the hypoconid is small and it is next to the distal wall of the protoconid where it reaches the crest on the distal face of the protoconid; labially, the hypoconid joins the accessory cuspid by a very short cristid. Distal to this accessory cuspid, the labial postcingulid emerges and borders the labial side of the talonid. The postcristid runs toward the base of the protoconid, closing the lingual side of the talonid. The two subtle cuspules observed in IBIGEO-P 110 at the lingual border of the talonid are absent in the type specimen.
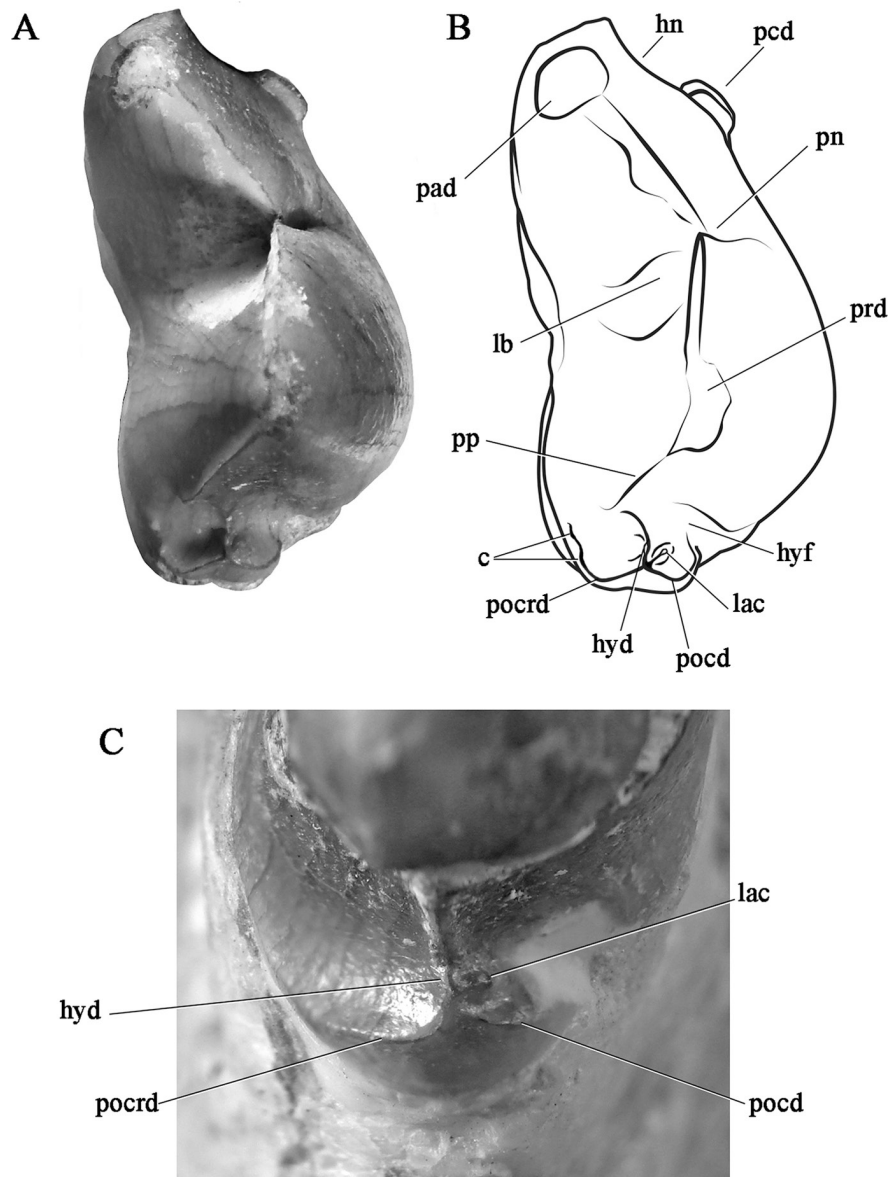
Figure 5. *Callistoe vincei*, right m4 in occlusal view in holotype (PVL 4187) and IBIGEO-P 110. **A** IBIGEO-P 110; **B** IBIGEO-P 110, line drawing; **C** distal view of the talonid of the type specimen PVL 4187. Abbreviations: **c** cuspulid; **hn** hypoconulid notch; **hyd** hypoconid; **hyf** hypoflexid; **lac** labial accessory cuspid; **lb** lingual basin; **pad** paraconid; **pcd** precingulid; **pn** paracristid notch; **pocd** labial postcingulid; **pocrd** postcristid; **pp** postprotocristid; **prd** protoconid. Teeth not at scale.

Description of mesowear facets in the lower dentition of *Callistoe vincei*

Two names taken from dentistry are often used to refer to tooth wear: abrasion, caused by the contact between food/dust/detritus and tooth; and attrition, wear caused by the contact between teeth (Butler 1952). Although both mechanisms are often combined during mastication, if abrasion is dominant the impressions within enamel are often rounded and have no clear marginal edges (Koenigswald 2018); attritional marks are distinguished by flat areas usually with striations parallel to the movement direction (Butler 1952). This last mechanism forms facets and sharps teeth, while abrasion blunts them (Ungar 2015).

The occlusal patterns and their impressions on the tooth surface were intensely studied from more than 100 years for several purposes, e.g., evolution of tribosphenic molar and study of cusp homology, direction of chewing movements, type of ingested diet (among a prolific literature, e.g., Osborn 1888; Butler 1952, 1971; Patterson 1956; Mills 1966; Crompton and Hiiemae 1970; Crompton 1971; Greaves 1973; Crompton and Kielan-Jaworowska 1978; Fortelius 1985; van Valkenburgh 1988; Lucas 2004; Teaford 2007; Davis 2011; Smits and Evans 2012; Ungar 2015; Koenigswald 2018; Schultz et al. 2018). In the following section we describe the mesowear facets in the lower dentition of *Callistoe*, using traditional works of Crompton (1971), Crompton and Kielan-Jaworowska (1978), and the more recent revision of Davis (2011).

The p1 exhibits a distolingual facet exposing a dentine core surrounded by an enamel border. Toward the crown base the wear affected a distolingual cingulid which remains as a subtle ridge (Fig. 3E).
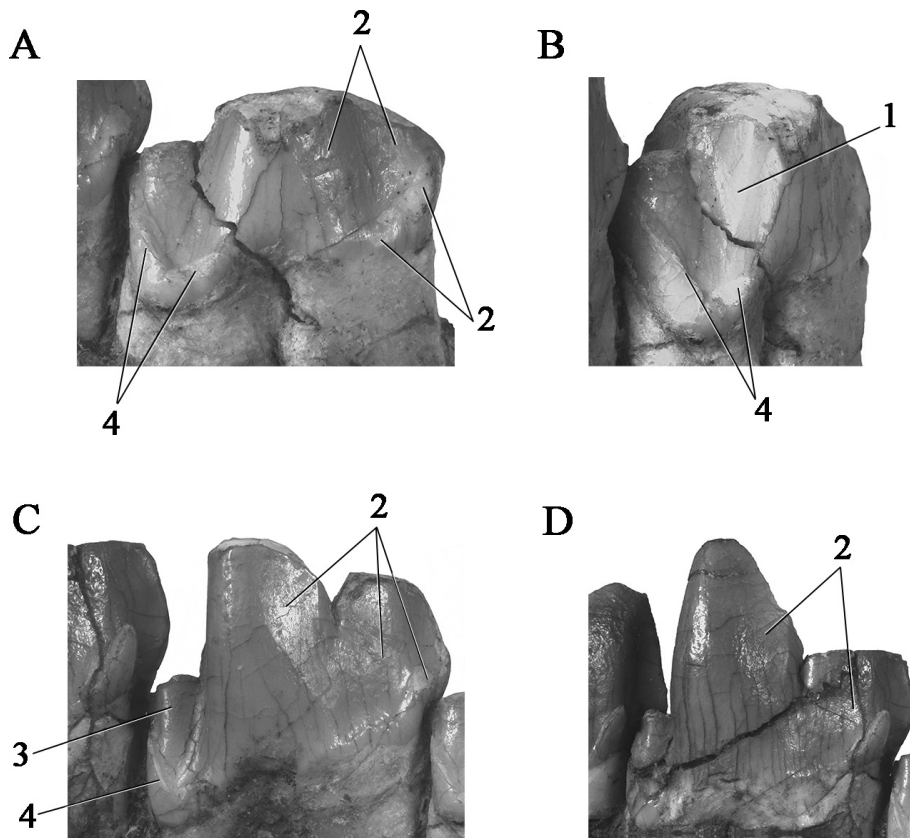
Figure 6. *Callistoe vincei* IBIGEO-P 110, attritional wear facets in m1 to m3. **A, B** m1 in labial and distal view, respectively; **C** m2 in labial view; **D** m3 in labial view. Abbreviations: **1, 2, 3, 4** attritional facets sensu Compton (1971). Teeth not at scale.

In the m1 the wear caused the loss of the paraconid and protoconid, remaining only the cusp bases (Fig. 6A, B). The exposed dentine surface is visible in occlusal view; it is surrounded by an enamel border. The labial side exhibits the remains of the cutting facet 2 of Crompton (1971), which on the m1 is brought about by the initial contact with the DP3 (a sectorial tooth in sparassodonts; Forasiepi and Sánchez-Villagra 2014) and in adult age with the distolingual side of the P3. In sparassodonts, the deciduous premolar is functional in juvenile specimens; this is particularly clear in *Arminiheringia* sp. (MLP 82-V-1-1) in which the m1 and m2 are heavily worn, while the P3 only exhibits facets restricted to the main cusp (Forasiepi and Sánchez-Villagra 2014). The facet 2 also includes the precingulid which exposes the dentine at the most mesial part. The wear facet 1 is restricted to the distolabial part of the distal face of the protoconid and appears to extend to the mesiolabial side of the talonid (Fig. 6B). It is formed by the contact with the paracingulum and paracone of the M1. The crown of the M1 is not preserved in other specimens of *Callistoe vincei* (the holotype and PVL 4207) but the paracingulum was probably present judging by its existence in the M3. On the labial side of the talonid, the postcingulid is barely worn down by an incipient contact with the mesiolingual face of the metacone of the M1 (facet 4 of Crompton 1971). The facet originated by the contact with the distolingual face of the paracone (facet 3 of Crompton 1971) is also present in this molar. There are no traces of lingual wear facets (5 and 6 of Crompton 1971) on the tal-

onid of this specimen. In the typical tribosphenic pattern these facets are brought about by the contact with the mesial and distal sides of the protocone, cusp which is much reduced in *Callistoe*. In the talonid, the apical wear areas caused by abrasion and identified as small rounded zones devoid of enamel, are restricted to the hypoconid and entoconid. Notably, in this specimen of *Callistoe vincei* the m1 is not as worn as in the juvenile specimen of *Arminiheringia* sp. (MLP 82-V-1-1), where the first molar is heavily worn out while the m4 is not yet completely erupted, suggesting that in MLP 82-V-1-1 the m1 probably erupted earlier than in *Callistoe*.

The m2 exhibits abrasion at the apex and mesial edge of the paraconid, the apex of the protoconid and upper third of the postprotocristid, the apex of hypoconid and entoconid, and the lingual side of the paracristid notch. Worn areas caused by attrition corresponds to facets 1, 2 (covering the paracristid, the labial wall of the trigonid and the precingulid), and 4 of Crompton (1971) (Fig. 6C); these are brought about by the contact with the paracingulum and mesial side of the paracone of the M2, postmetacrista of the M1, and the mesiolingual face of the metacone of the M2, respectively. Moreover, on the mesiolabial slope of the hypoconid the facet 3 is clearly present, formed by the contact with the distal face of a reduced paracone of the M2. As in the m1, there is a considerable difference in the degree of wear between the m2 of *Callistoe* IBIGEO-P 110 and the juvenile *Arminiheringia* sp. (MLP 82-V-1-1), where the second lower molar lost almost the entire crown.

On the m3, the contact between food and tooth —abrasion— is visualized as facets on the paraconid, lingual side of the paracristid and postprotocristid, paracristid notch, and the apex of the metaconid and hypoconid. The attritional facets are feeble, i.e., did not cause complete enamel denudation. They are represented by Crompton's facet 1 identified as a vertical and planar surface on the distal face of the protoconid, facet 2 (mainly on the labial face of preprotocristid and precingulid), and facet 3, poorly developed and restricted to the apical portion of the labial slope of the hypoconid (Fig. 6D).

The m4 is the tooth less affected by wear. The abrasion is limited to the most apical portion of the paraconid and protoconid, the lingual side of paracristid and base of the paracristid notch, and the lingual border of the postprotocristid. Attritional facets are facet 1, seen as a thin band on the distolabial portion of the protoconid and facet 2, restricted to the preprotocristid. The talonid was not affected by wear.

Discussion

The new material here studied is assigned to the species *Callistoe vincei* based on of similarities in the morphology of the canine (several longitudinal striae, sulci, and grooves extended along the entire length of the canine, and enamel layer extremely thin that desappears in advanced wear stages) and in the morphology of the m4 present in the holotype (PVL 4187). The m4 is characterized by an enlarged trigonid with paraconid and protoconid, and reduced and unbasined talonid bearing a labial accessory cuspid linked with the hypoconid (type specimen) or with the distal border of the talonid (IBIGEO-P 110). Moreover, the relative dental and mandibular proportions are also similar between the type and IBIGEO-P 110 specimens. These similar traits, in addition to the fact that both the holotype, the specimen PVL 4207, and IBIGEO-P 110 come from the same stratigraphic and geographic provenance, indicate that the new specimen here studied is part of the hypodigm of *Callistoe vincei*.

The discovery of IBIGEO-P 110 specimen of *C. vincei* allows the recognition of unusual features of the lower dental anatomy in derived sparassodonts. In particular, the retention of character states considered primitive, such as the presence of the metaconid and a basined talonid with a complete set of plesiomorphic cusps: hypoconid, hypoconulid, and entoconid.

In the context of the phylogeny of Sparassodonta, the distribution of the metaconid is homoplastic, being present in non-closely related forms. Among basal taxa, *Patene* and *Stylocynus* are the only genera where the metaconid is certainly present in the complete molar series (Marshall 1979; Marshall 1981; Babot and Ortiz 2008; Rangel et al. 2019). *Nemolestes* is an other basal sparassodont bearing metaconid (Marshall 1978; Forasiepi et al. 2015). Although the genus is represented by isolated lower molars not certainly associated with any particular

locus, given the primitive nature of the known molars, we infer in this taxon the presence of a metaconid on the complete molar series. This assumption is also valid for *Hondadelphys*, another basal Sparassodonta, in which the metaconid is present in the m2–4 but the condition in the m1 is unknown (Marshall 1976; Suárez 2019). In Hathlyacynidae, the metaconid is absent in all molars, as is in the case of some basal Borhyaenoidea like *Prothylacynus* and *Pseudothylacynus* (Forasiepi et al. 2015; Engelman et al. 2018). Other stem Borhyaenoidea, such as *Plesiofelis*, *Chlorocyon*, and *Pharsophorus*, exhibit a small metaconid on the m2–4 (Forasiepi et al. 2015; Engelman et al. 2018), and it is also the condition in *Lycopsis longirostrus* (Suárez 2019). In distal Borhyaenoidea, e.g., the family Borhyaenidae, the metaconid is present on m2–m3 in *Artodictis sinclairi*, present on the m2–4 in *Australohyaena*, and exhibits intraspecific variation in *Borhyaena*, where it is absent in the m1, present in the m2 and m3, but variably present on the m4 (Forasiepi 2009; Forasiepi et al. 2015; Engelman et al. 2018). Among thylacosmilids, in *Anachlysictis* the metaconid is absent on the m2–4 (the condition of the m1 is unknown) and *Thylacosmilus* lacks a metaconid (Suarez 2019). In *Arminiheringia auceta* (type specimen MACN-A 10970) the metaconid is not visible —the molar series is very affected by wear obscuring observation, and in *Proborhyaena* (AMNH 29576) it is absent in all molars.

The homology of the metaconid in the family Borhyaenidae was treated in detail in Forasiepi et al. (2015) who proposed that the cusp distal to the protoconid in m2–4 is homologous to the metaconid, given the connection of this last cups and the protoconid by a notched crest, interpreted by these authors as a postprotocristid. Conversely, the cusp distal to the protoconid in the m1 was considered as a hypoconid, based on the topological relationship with the other cusps of the talonid.

The unique condition observed in the specimen IBIGEO-P 110 adds new variation in the trigonid cusp arrangement in Sparassodonta: a metaconid present in the m3 and absent in the m2 and m4 (the condition in the m1 is unknown). In *Callistoe*, contrary to the pattern described for Borhyaenidae, the position of the metaconid is lingual to the protoconid, maintaining a plesiomorphic topology present in basal sparassodonts and in the m2 and m3 of *Pharsophorus*. The presence/absence of a postprotocristid notch correlated with the presence/absence of a metaconid, regardless of its size, shows that the portion of the postprotocristid lingual to the notch is under the control of the metaconid and dependent likely under the influence of a secondary enamel (metaconid) knot. Similar control of cusp and overall crown morphology is known to be present in living mammals, were a relatively simple cusp pattern is controlled by inhibitory cascades (Jernvall 2000; Savriama et al. 2018). *Callistoe* is surprising in preserving the plesiomorphic pattern of a distinct metaconid and labial extension into a postprotocristid notch only in the m3. Assuming that the cusp is absent in the m1 as is certainly the case of the m2, the simplest explanation is that the expression of the derived character (disappearance of the metaconid and related structures) advances

posteriorly. The m1 should be the first erupting molar and the most precocious one, followed by the m2 and the m3, where the morphology is still plesiomorphic. The molars would reflect a morphological and evolutionary gradient of character change. The absence of the metaconid in the m4 can be conceived as related to the functional reduction of the distal half of the lower molar in taxa with an equal number of upper and lower molariforms and the developmental factors controlling molar size gradient (Vitek et al. 2020). In addition to the plesiomorphic retention of the metaconid, in *Callistoe* the talonid in the m1–3 (unknown until the discovery of the specimen IBIGEO-P 110), also conserves a plesiomorphic pattern composed by distinct hypoconid, entoconid, hypoconulid, and a well-delimited, thought small, basin. This pattern is present in basal and small and medium-size sparassodonts (*Patene*, *Nemolestes*, *Hondadelphys*, *Stylocynus*) but is also present in the large *Arminiherigia auceta*. Here, a tricuspidated talonid is present at least on the m2–3.

Palaeoecological interpretation of molar morphology in *Callistoe*

Despite the presence of a typical tribosphenic arrangement in the talonid (cuspids + basin), this structure in *Callistoe* is reduced, very low in relation to the trigonid and does not act as a functionally significant crushing basin.

The non-functional talonid basin is supported by the low relative grinding area (RGA) calculated for *Callistoe* (RGA = < 0.17) which is congruent with the values derived from extant hypercanivorous mammals (van Valkenburg 1991; Zimicz 2012; Croft et al. 2018) and also in the range of RGA interpreted for several Borhyaenoidea and Hathliacynidae (Prevosti et al. 2013; Croft et al. 2018). Distal to the trigonid, the functional area is the labial cutting edge of the talonid which involves the contact with the distal face of the reduced paracone and the mesial face of the metacone with the mesial and distal side of the hypoconid (facets 3 and 4 of Crompton 1971). In more advanced wear stages —represented by the type specimen PVL 4187—, the labial wall of the talonid becomes a marked vertical facet, denuding the labial side of the hypoconid and the labial postcingulid, but not affecting the structures lingual to the hypoconid. This pattern is mainly visible in the two last molars as well as in other large sparassodonts such as *Arminiheringia*, *Proborhyaena*, *Arctodictis*, and *Australohyaena*.

Other dental morphometric indices that support a hypercarnivorous diet for *Callistoe* are those considered by Zimicz (2012) and Prevosti et al. (2013), and modified from van Valkenburgh (1989, 1991), Werdelin (1989), and Palmqvist et al. (2011). These are the premolar shape (PS, width of p3/length of p3; *Callistoe* = 0.53) and the relative premolar size (RPS, width of p3/cube root of body mass in kg; *Callistoe* = 1.63). The PS and RPS indices suggest fleshy items as principal components of the diet, and reflect the labiolingual compression of the third premolar in *Callistoe*, which does not seem a tooth adapted to resist hard foods. This condition is also present

in basal Borhyaenoidea (e.g., *Prothylacynus*, *Lycopsis*), *Arminiheringia* sp. (MLP 82-V-1-1) and contrasts with the inflated aspect of the p3 in, e.g., Borhyaenidae, *Australohyaena*, *Proborhyaena* cf. *P. gigantea* (MNHN-DP 720); the latter morphology was largely associated with durophagy by several studies (Zimicz 2012; Prevosti et al. 2013; Forasiepi et al. 2015). Another diet predictor index is the relative premolar length (RPL) which quantifies the length of the largest premolar in relation to the length of the largest molar (van Valkenburgh 1990; Palmqvist et al. 2011; Zimicz 2014). In *Callistoe* the RPL (= 0.57) falls in the range of mesocarnivores (mammals that consume mainly meat but also insects and other invertebrates; van Valkenburgh 1989). This value would imply the use of lingual areas of the talonid to crush small soft bodies and exoskeleton pieces, of which there is no evidence in the lower molars of *Callistoe*. As remarked by Engelman et al. (2020), the predictive value of this index in metatherians should be reconsidered because extant Australian hypercarnivorous marsupials also fall in the range of mesocarnivorous mammals under the RPL parameter.

Among carnivorous extant taxa, a widely applied parameter to discriminate the meat content in diet is the relative blade length (RBL) which measures the blade development in the carnassial lower molar (van Valkenburgh 1989). Following this author, RBL >1 defines extant Felidae which predominant diet is based on meat. *Callistoe* (RBL = 0.90) does not fall strictly in this category but is close to meat and meat/bone eater values, as was inferred for several sparassodonts (see Zimicz 2012; Forasiepi et al. 2015; Croft et al. 2018; but also see Engelman et al. 2020). In summary, the parameters examined above in *Callistoe vincei* indicate that this species was a hypercarnivorous form, whose diet was mainly based on fleshy items. However, we do not discard osseous elements as an eventual component of the diet. This hypothesis, originally advanced at a time when the details of its dental morphology were largely unknown (Babot et al. 2002), was based on the mandibular shape, which reveals a relatively common morphospace among extant durophagous placental and marsupials and some of the largest sparassodonts (Echarri et al. 2017; Croft et al. 2018).

Lower molar wear in *Callistoe*

The development of wear facets in mammalian teeth is conditioned by the initial shape of the occlusal surface, the type of enamel, the initial distribution of enamel and dentine in the occlusal surface, the type of diet and habitat, the eruption pattern, and the tooth position in the dental row (Fortelius 1987; Kaiser and Schulz 2006; Kullmer et al. 2009; Taylor et al. 2013; Schultz et al. 2018). Fortelius (1985) divided the mammalian tooth crown shape in primary and secondary occlusal surfaces. The first category includes teeth that use the initial enamel cover as soon as a tooth erupts; the crown deteriorates gradually, forms flat areas with dentine surrounded by enamel, and in later stages the tooth remains as a dentine knob. In the second category, the teeth develop a secondary and functionally efficient occlusal surface once some initial wear

with antagonist pieces has occurred. The new facets expose part of dentine and the sections formed by enamel and dentine (enamel band; Koenigswald 2018) are the functional structures. In this last category, Koenigswald (2018) includes, among others, the carnassial teeth of most eutherian and some metatherian carnivorous forms. In these cases, the facet has a blade-like design, symmetrical between antagonists, and defined by a flat enamel band where both components are continuous and set in an almost vertical position.

In Sparassodonta, the first mention related to the enamel type, wear, and occlusion patterns appeared in Marshall (1978) who superficially related the thin nature of the enamel in sparassodonts (especially in Proborhyaeninae, sensu Marshall 1978), with the tooth susceptibility to extreme wear and its effects on occlusion. Later, Koenigswald and Goin (2000) studied the enamel microstructure of several South American metatherians and identified the main enamel feature of some sparassodont species. One particular feature in *Arminiheringia* and *Proborhyaena* is the enamel thinness, in relation to smaller members of the group but also to other placental and marsupial carnivorous genera. This distinctive feature inhibits the development of long-lasting secondary wear facets, i.e., in these teeth the self-sharpening enamel band —cross section of enamel and dentine— does not form. This is also the case in Dasyuridae and Thylacinidae (Koenigswald and Goin 2000).

In *Callistoe* the cutting edge on lower molars also has an ephemeral functional stability; the trigonid secondary blade-like facet fails to form; the very thin enamel layer lingual to the paracristid probably accelerated the denudation of the crown because when the labial enamel cover was lost, the lingual side worn down even faster. Once the dentine knob was formed, the cutting function is replaced by the posterior sectorial teeth, given the homodont condition of the carnassial complex in Sparassodonta (Koenigswald and Goin 2000). In the new specimen of *Callistoe* here studied, all the molars, except m1, preserve the cutting edge, but in the type specimen (PVL 4187) it is only present in the m4. Marshall (1978) considered that in *Arminiheringia* the dentine stump resulting after the initial molar profile disappears, would have retained its functionality judging by the striations on the surface. This could be also valid for *Callistoe*, although these striations are not visible under magnified binocular observation in the molars with advanced wear. The function in heavy worn teeth in both, *Callistoe* and *Arminiheringia*, would have been restricted to hold food and/or contributed to disaggregate ingested items already processed by the functional molars preserving the cutting edges. As already mentioned, in *Callistoe* the talonid develops a functional facet (Crompton's facets 3 and 4; see Fig. 6) that sharpens the labial side of the tooth and remains as a vertical cutting edge, even in advanced wear stages.

The obliteration of the molar crown generates a gap and the interruption of the occlusal contact, reducing the effectiveness in food treatment and related biological consequences (Ungar 2005, 2010). In order to maintain the contact between wear antagonist, the teeth erupt throughout life via compensatory process known as supraeruption, overeruption, or hypereruption, mainly defined in the case of loss of teeth in humans and but also valid to explain the persistence of the occlusal function in heavy wear teeth (Craddock and Youngson 2004 and references; see Kaifu et al. 2003 for ancient human populations). Studies focused on wild mammals are rare, although some works use tooth wear and overeruption proxies for age determination analysis (Jones et al. 2008; Pollock et al. 2021). In the alveolar region, this process is detected by an increase of the distance between the CEJ and the alveolar edge and the consequent root denudation (Danenberg et al. 1991).

In many large sparassodonts the great size of premolar and molar roots is noteworthy, as is their exposure over the alveolar border. This feature, present in e.g., *Borhyaena*, *Australohyaena*, *Pharsophorus*, is even more conspicuous in *Proborhyaena*, *Arminiheringia*, and *Callistoe*. In some specimens of these genera, the molars show a particular arrangement: in the mesial and more worn molars the distance between the CEJ and the inter-radicular septum is longer than in the less worn posterior teeth. This pattern is evident in, e.g., the labial side of right pairs M2 and M3 and m3 and m4 in the type specimen of *Callistoe* (PVL 4187; Fig. 1B), the m1 and posterior molars in the IBIGEO specimen (Fig. 5A, B), as well as in the holotype of *Arminiheringia* (MACN-A 10970), and *Proborhyaena* cf. *P. gigantea* (MNHN-DP 720). This arrangement could be explained by compensatory overeruptive process performed to maintain the occlusal distance among antagonist teeth heavily affected by wear.

In *Callistoe*, other functional lower teeth effective for meat processing besides molars, are the enlarge canines and third premolars. As explained above, in the lower canine of *Callistoe* the enamel is restricted to the apical part which is lost at the initial stages of wear. In this hypercarnivorous form, the canines maintain the functionality by their hypsodont condition. Following Koenigswald (2011, 2018), this kind of canine is a dentine hypsodont tooth formed by a heterochronic process in which one of the last stages of tooth development after eruption —loss of enamel and dentine persistence— is prolonged. In this type of teeth dominated by dentine, if the enamel is present, it is functionally immaterial. As shown in Babot et al. (2002), the lower canine roots are opened in the adult specimens of *Callistoe*, *Arminiheringia*, and *Proborhyaena*, as a consequence of heterochronic delay in root formation (Madden 2015); the presence of closed roots in an upper canine of a senile individual of cf. *Proborhyaena* suggests that this genus was not euhypsodont, i.e., fully ever-growing, condition that could be also present in old individuals of the related genera *Callistoe*, *Arminiheringia*, and *Paraborhyaena* (Babot et al. 2002; Forasiepi and Sánchez-Villagra 2014).

Based on Forasiepi and Sánchez-Villagra (2014), the eruption sequence observed in *Arminiheringia* sp. MLP 82-V-1-1 suggests that the p3 erupts slightly before the last molar, a condition that could be also present in *Callistoe*. In the holotype PVL 4187, the p3 and the m4 show a similar degree of wear; both teeth —mainly the right

ones— are worn on mesial, labial, and apical areas but preserve the crown almost complete, while p1, p2 and m1–3, are strongly worn. In older individuals of the related species *Arminiheringia auceta* (holotype MACN-A 10970) the crown of the third premolar was lost, and therefore the only functional teeth for meat processing are the canine and the m4. The tooth morphology, the low enamel quality, and the associated wear pattern in these closely related Eocene carnivorous species could have play an important role in diminishing the functional efficiency of teeth, the nutritional value of food, and ultimately the reproductive fitness, as has been well studied in extant mammals (Ungar 2015).

Conclusions

The new specimen of *Callistoe vincei* presented here reveals characters seldom recorded in the lower dentition of large Sparassodonta. Even though *Callistoe* is one of the best preserved Paleogene sparassodonts, the lower dental series was not fully conserved in the type (PVL 4187). The new material represents a young adult, with the molar series completely erupted but with few signs of wear on the posterior molars. At this ontogenetic phase the associated canine exhibits enamel restricted to the apical portion. The m2–4 were completely preserved, showing unexpected features in the lower molars of this derived species, such as the presence of a metaconid only in the m3, and hypoconid, hypoconulid, and entoconid in the talonid in m1–3. The retention of a metaconid in a molar and a full complement of talonid cusps emphasizes the enduring retention of these plesiomorphic traits even among deeply nested and derived sparassodonts and the repeated and independent loss of these generalized features in lineages emphasizing carnivory or hypercanivory. The wear facets due to abrasion are located at the cuspid tips, the lingual and basal side of the paracristid notch, and the lingual edge of the postprotocristid; those generated by attrition are restricted to the labial wall of the tooth (both on the trigonid as well on the talonid), as expected for mammalian carnivorous forms. The structures affected by attrition are the precingulid, the paracristid, the distolabial slope of the protoconid, and the labial side of the talonid, including the hypoconid and the labial postcingulid. In contrast to several extinct and extant Carnivora and some marsupial carnivorous forms, in *Callistoe* the molars do not form a self-sharpening facet, as already mentioned for other large hypercarnivorous sparassodonts. The attritional facet 2 (in terms of Crompton 1971) is ephemeral because the extreme thinness of the enamel on the lingual side of the paracristid notch, triggers a rapid denudation of the paraconid and protoconid. Instead, the talonid does develop a labial vertical sharp functional facet, which remains as a cutting edge even in later wear stages. Given the wear conditions of the trigonid, overeruption —exposure of tooth roots over the alveolar edge— could have been a mechanism to maintain the occlusal contact between antagonist teeth. From a functional point of view, the new specimen presented here supports previous dietary inferences related with hypercarnivory in *Callistoe*. In the adult life stage, the only teeth involved in carnivory in this genus were the hypsodont canines, the third premolars and the m3/m4 or only the m4.

Author contribution

Judith Babot: Conceptualization, investigation, methodology, writing original draft – review, visualization, writing – review and editing; Guillermo Rougier: Conceptualization, investigation, writing original draft; writing – review and editing; Daniel García-López: Investigation, writing – review and editing, visualization; Virginia Deraco: writing – review and editing; Claudia Herrera: Writing – review and editing; Sara Bertelli: Funding acquisition and project administration, visualization; writing – review and editing; Norberto P. Giannini: Writing – review and editing, Funding acquisition and project administration, writing – review and editing.

Competing interests

The authors have declared that no competing interests exist.

Acknowledgements

References

Anders U, Koenigswald WV, Ruf I, Smith BH (2011) Generalized individual dental age stages (IDAS) for fossil and extant placental mammals. Palaontologische Zeitschrift 85: 321–339. https://doi.org/10.1007/s12542-011-0098-9

Ameghino F (1887) Enumeración sistemática de las especies de ma-míferos fósiles coleccionados por Carlos Ameghino en los terrenos eocenos de la Patagonia Austral y depositados en el Museo de La Plata. Boletín del Museo de La Plata 1: 1–26.

Argot C, Babot MJ (2011) Postcranial morphology, functional adaptations and palaeobiology of *Callistoe vincei*, a predaceous metatherian from the Eocene of Salta, north-western Argentina. Palaeontology 54: 447–480. https://doi.org/10.1111/j.1475-4983.2011.01036.x

Babot MJ (2005) Los Borhyaenoidea (Mammalia, Metatheria) del Terciario inferior del Noroeste argentino. Aspectos filogenéticos, paleobiológicos y bioestratigráficos. PhD Thesis, Universidad Nacional de Tucumán, Tucumán, Argentina, 454 pp.

Babot MJ, Ortiz PE (2008) Primer registro de Borhyaenoidea (Mammalia, Metatheria, Borhyaenoidea) de la provincia de Tucumán. Acta geológica lilloana 21: 34–48. http://www.lillo.org.ar/journals/index.php/acta-geologica-lilloana/article/view/21 [Accessed on 22.02.2022]

Babot MJ, Powell JE, Muizon C (2002) *Callistoe vincei*, a new Proborhyaenidae (Borhyaenoidea, Metatheria, Mammalia) from the early Eocene of Argentina. Geobios 35: 615–629. https://doi.org/10.1016/s0016-6995(02)00073-6

Blanco RE, Jones WW, Grinspan GA (2011) Fossil marsupial predators of South America (Marsupialia, Borhyaenoidea): Bite mechanics and palaeobiological implications. Alcheringa 35: 377–387. https://doi.org/10.1080/03115518.2010.519644

Butler PM (1952) The milk-molars of Perissodactyla with remarks on molar occlusion. Proceedings of the Zoological Society of London B 121: 777–817. https://doi.org/10.1111/j.1096-3642.1952.tb00784.x

Butler PM (1971) Some functional aspects of molar evolution. Evolution 26: 474–483. https://doi.org/10.2307/2407021

Craddock HL, Youngson CC (2004) Eruptive tooth movement – the current state of knowledge. British Dental Journal 197: 385–391. https://doi:10.1038/sj.bdj.4811712

Croft DA, Engelman RK, Dolgushina T, Wesley G (2018) Diversity and disparity of sparassodonts (Metatheria) reveal non-analogue nature of ancient South American mammalian carnivore guilds. Proceedings of the Royal Society B: Biological Sciences 285: 20172012. http://doi.org/10.1098/rspb.2017.2012

Crompton AW (1971) The origin of the tribosphenic molar. In: Kermack DM, Kermack KA (Eds) Early Mammals. Zoological Journal of the Linnean Society 50 Suppl 1: 65–87.

Crompton AW, Hiiemae KM (1970) Molar occlusion and mandibular movements during occlusion in the American opossum, *Didelphis marsupialis*. Zoological Journal of the Linnean Society 49: 21–47.

Crompton AW, Kielan-Jaworowska Z (1978) Molar structure and occlusion in Cretaceous therian mammals. In: Butler PM, Josey KA (Eds) Studies in the Development, Function and Evolution of the Teeth. Academic Press, New York, 249–287.

Danenberg PJ, Hirsch RS, Clarke NG, Leppard PI, Richards LC (1991) Continuous tooth eruption in Australian aboriginal skulls. American Journal of Physical Anthropology 85: 305–12. https://doi.org/10.1002/ajpa.1330850309

Davis BM (2011) Evolution of the tribosphenic molar pattern in early mammals, with comments on the "Dual-Origin" hypothesis. Journal of Mammalian Evolution 18: 227–244. https://doi.org/10.1007/s10914-011-9168-8

del Papa C, Kirschbaum A, Powell J, Brod A, Hongn F, Pimentel M (2010) Sedimentological, geochemical and paleontological insights applied to continental omission surfaces: a new approach for reconstructing an Eocene foreland basin in NW Argentina. Journal of South American Earth Sciences 29: 327–345. https://doi.org/10.1016/j.jsames.2009.06.004

del Papa CE, Babot MJ, Dahlquist J, García-López DA, Deraco V, Herrera CM, Bertelli S, Rougier GW, Giannini NP (2022) Toward a chronostratigraphy of the Paleocene-Eocene sedimentary record in Northwestern Argentina. Journal of South American Earth Science 113. https://doi.org/10.1016/j.jsames.2021.103677

Diogo R., Bello-Hellegouarch, G, Kohlsdorf T, Esteve-Altava B, Molnar JL (2016) Comparative myology and evolution of marsupials and other vertebrates, with notes on complexity, bauplan, and "Scala Naturae". Anatomical Record 299: 1224–1255. https://doi.org/10.1002/ar.23390

Echarri S, Ercoli MD, Chemisquy MA, Turazzini G, Prevosti JF (2017) Mandible morphology and diet of the South American extinct metatherian predators (Mammalia, Metatheria, Sparassodonta). Earth and Environmental Science Transactions of the Royal Society of Edinburgh 106: 277–288. https://doi.org/10.1017/S1755691016000190

Engelman RK, Croft DA (2014) A new species of small-bodied sparassodont (Mammalia, Metatheria) from the middle Miocene locality of Quebrada Honda, Bolivia. Journal of Vertebrate Paleontology 34: 672–688. https://doi.org/10.1080/02724634.2013.827118

Engelman RK, Flynn JJ, Wyss AR, Croft DA (2020) *Eomakhaira molossus*, a new saber-toothed sparassodont (Metatheria: Thylacosmilinae) from the Early Oligocene (?Tinguiririran) Cachapoal Locality, Andean Main Range, Chile. American Museum Novitates 3957: 1–75. https://doi.org/10.1206/3957.1

Engelman RK, Flynn JJ, Gans P, Wyss AR, Croft DA (2018) *Chlorocyon phantasma*, a late Eocene borhyaenoid (Mammalia: Metatheria: Sparassodonta) from the Los Helados locality, Andean Main Range, Central Chile. American Museum Novitates 3918: 1–22. https://doi.org/10.1206/3918.1

Ercoli MD, Álvarez A, Busker F, Morales MM, Julik E, Smith HF, Adrian B, Barton M, Bhagavatula K, Poole M, Shahsavan M, Wechsler R, Fisher RE (2017) Myology of the head, neck, and thoracic region of the lesser grison (*Galictis cuja*) in comparison with the red panda (*Ailurus fulgens*) and other carnivorans: Phylogenetic and functional implications. Journal of Mammalian Evolution 24: 289–322. https://doi.org/10.1007/s10914-016-9339-8

Evans AR (2005) Connecting morphology, function and tooth wear in microchiropterans. Biological Journal of the Linnean Society 85: 81–96. https://doi.org/10.1111/j.1095-8312.2005.00474.x

Evans HE, de Lahunta A (2013) Miller's Anatomy of the Dog. Elsevier Saunders, St Louis, Missouri, 871 pp.

Fernicola JC, Zimicz AN, Chornogubsky L, Ducea M, Cruz LE, Bond M, Arnal M, Cárdenas M, Fernández M (2021) The Early Eocene Climatic Optimum at the Lower Section of the Lumbrera Formation (Ypresian, Salta Province, Northwestern Argentina): Origin and early diversification of the Cingulata. Journal of Mammalian Evolution 28: 621–633. https://doi.org/10.1007/s10914-021-09545-w

Forasiepi AM (2009) Osteology of *Arctodictis sinclairi* (Mammalia, Metatheria, Sparassodonta) and phylogeny of Cenozoic metatherian carnivores from South America. Monografías del Museo Argentino de Ciencias Naturales 6: 1–174.

Forasiepi AM, Sanchez-Villagra MR (2014) Heterochrony, dental ontogenetic diversity, and the circumvention of constraints in marsupial mammals and extinct relatives. Paleobiology 40: 222–237. https://doi.org/10.1666/13034

Forasiepi AM, Babot MJ, Zimicz AN (2015) *Australohyaena antiqua* (Mammalia, Metatheria, Sparassodonta), a large predator from the

late Oligocene of Patagonia. Journal of Systematic Palaeontology 13: 505–523. https://doi.org/10.1080/14772019.2014.926403

Fortelius M (1985) Ungulate cheek teeth: development, functional, and evolutionary interrelations. Acta Zoological Fennica 180: 1–76. http://www.rhinoresourcecenter.com/pdf_files/139/1396052224.pdf [Accessed on 22.02.2022]

Fortelius M (1987) A note on the scaling of dental wear. Evolutionary Theory 8: 73–75. https://www.mn.uio.no/cees/english/services/van-valen/evolutionary-theory/volume-8/vol-8-no-2-pages-73-75-m-fortelius-a-note-on-the-scaling-of-dental-wear.pdf [Accessed on 22.02.2022]

Greaves WS (1973) The inference of jaw motion from tooth wear facets. Journal of Paleontology 47: 1000–1001. http://www.jstor.org/stable/1303088 [Accessed on 22.02.2022]

Hiiemae K, Jenkins FA (1969) The anatomy and internal architecture of the muscles of mastication in *Didelphis marsupialis*. Postilla 140: 1–49.

Jernvall J (2000) Linking development with generation of novelty in mammalian teeth. Proceeding of the National Academy of Sciences 97: 2641–2645. https://doi.org/10.1073/pnas.050586297

Jones ME, Cockburn A, Hamede R, Hawkins C, Hesterman H, Lachish S, Mann D, McCallum H, Pemberton D (2008) Life-history change in disease-ravaged Tasmanian devil populations. Proceedings of the National Academy of Sciences 105: 10023–10027. https://doi.org/10.1073/pnas.0711236105

Kaifu Y, Kasai K, Townsend GC, Richards LC (2003) Tooth wear and the "design" of the human dentition: a perspective from evolutionary medicine. American Journal of Biological Anthropology, Supplement 37: 47–61. https://doi.org/10.1002/ajpa.10329

Kaiser TM, Schulz E (2006) Tooth wear gradients in zebras as an environmental proxy – a pilot study. Mitteilungen aus dem Hamburgischen Zoologischen Museum und Institut 103: 187–210.

Koenigswald W von (2011) Diversity of hypsodont teeth in mammalian dentitions – construction and classification. Palaeontographica Abteilung A 294: 63–94.

Koenigswald W von (2018) Specialized wear facets and late ontogeny in mammalian dentitions. Historical Biology 30: 7–29. https://doi.org/10.1080/08912963.2016.1256399

Koenigswald W von, Goin FJ (2000) Enamel differentiation in South American marsupials and a comparison of placental and marsupial enamel. Palaeontographica Abteilung A 255: 129–168.

Kullmer O, Benazzi S, Fiorenza L, Schulz D, Bacso S, Winzen O (2009) Technical note: occlusal fingerprint analysis: quantification of tooth wear pattern. American Journal of Physical Anthropology 139: 600–605.

Lucas PW (2004) Dental Functional Morphology: How Teeth Work. Cambridge University Press, Cambridge, 355 pp. https://doi.org/10.1017/CBO9780511735011

Madden RH (2015) Hypsodonty in Mammals: Evolution, Geomorphology, and the Role of Earth Surface Processes. Cambridge University Press, Cambridge, UK, 423 pp.

Marshall LG (1976) New didelphine marsupials from the La Venta fauna (Miocene) of Colombia, South America. Journal of Paleontology 50: 402–418. http://www.jstor.org/stable/1303521 [Accessed on 22.02.2022]

Marshall LG (1978) Evolution of the Borhyaenidae, extinct South American predaceous marsupials. University of California Publications in Geological Sciences 117: 1–89.

Marshall LG (1979) Review of the Prothylacyninae, an extinct subfamily of South American "dog-like" marsupials. Fieldiana Geology

(new series) 3: 1–49. https://archive.org/details/reviewofprothyla-03mars [Accessed on 22.02.2022]

Marshall LG (1981) Review of the Hathlyacyninae, an extinct subfamily of South American "dog-like" marsupials. Fieldiana Geology (new series) 7: 1–120. https://ia902609.us.archive.org/0/items/reviewofhathlyac07mars/reviewofhathlyac07mars.pdf [Accessed on 22.02.2022]

Marshall LG, Case JA, Woodburne MO (1990) Phylogenetic relationships of the families of marsupials. In: Genoways HH (Ed) Current Mammalogy. Plenum Press, New York, 2: 433–505.

Mills JRE (1966) The functional occlusion of the teeth of Insectivora. Zoological Journal of the Linnean Society 46: 1–25. https://doi.org/10.1111/j.1096-3642.1966.tb00081.x

Muizon C de (1998) *Mayulestes ferox*, a borhyaenoid (Metatheria, Mammalia) from the early Paleocene of Bolivia. Phylogenetic and paleobiologic implications. Geodiversitas 20: 19–142.

Muizon C de, Ladevèze S (2020) Cranial anatomy of *Andinodelphys cochabambensis*, a stem metatherian from the early Palaeocene of Bolivia. Geodiversitas 42: 597–739. https://doi.org/10.5252/geodiversitas2020v42a30

Muizon C de, Cifelli RL, Céspedes Paz R (1997) The origin of the dog-like borhyaenoid marsupials of South America. Nature 389 (6650): 486–489. https://doi.org/10.1038/39029

Muizon C de, Ladevèze S, Selva C, Vignaud R, Goussad F (2018) *Allqokirus australis* (Sparassodonta, Metatheria) from the early Paleocene of Tiupampa (Bolivia) and the rise of the metatherian carnivorous radiation in South America. Geodiversitas 40: 363–459. https://doi.org/10.5252/geodiversitas2018v40a16

Osborn HF (1888) The evolution of mammalian molars to and from the tritubercular type. American Naturalist 22: 1067–1079.

Palmqvist P, Martínez-Navarro B, Pérez-Claros JA, Torregrosa V, Figuerido B, Jiménez-Arenas JM, Patrocinio Espigares M, Ros-Montoya S, De Renzi M (2011) The giant hyena *Pachycrocuta brevirostris*: modelling the bone-cracking behavior of an extinct carnivore. Quaternary International 243: 61–79. https://doi.org/10.1016/j.quaint.2010.12.035

Pascual R, Bond M, Vucetich MG (1981) El subgrupo Santa Bárbara (Grupo Salta) y sus vertebrados. Cronología, paleoambientes y paleobiogeografía. Octavo Congreso Geológico Argentino, San Luis, Argentina. Asociación Geológica Argentina 3: 743–758.

Patterson B (1956) Early Cretaceous mammals and the evolution of mammalian molar teeth. Fieldiana 13: 1–105. https://www.biodiversitylibrary.org/item/21537#page/19/mode/1up [Accessed on 22.02.2022]

Powell JE, Babot MJ, García-Lopez DA, Deraco MV, Herrera CM (2011) Eocene vertebrates of northwestern Argentina: annotated list. In: Salfity JA, Marquillas RA (Eds) Cenozoic Geology of the Central Andes of Argentina. SCS Publisher, Salta, Argentina, 349–370.

Pollock TI, Parrott ML, Evans AR, Hocking DP (2021) Wearing the devil down: Rate of tooth wear varies between wild and captive Tasmanian devils. Zoo Biology 40: 444–457. https://doi.org/10.1002/zoo.21632

Prevosti FJ, Forasiepi AM, Zimicz AN (2013) The evolution of the Cenozoic terrestrial mammal guild in South America: competition or replacement? Journal of Mammalian Evolution 20: 3–21. https://doi.org/10.1007/s10914-011-9175-9

Prevosti FJ, Forasiepi AM (2018) Evolution of South American Mammalian Predators During the Cenozoic: Palaeobiogeographic and Palaeoenvironmental Contingencies. Springer, Cham–Switzerland, 137–154. https://doi.org/10.1007/978-3-319-03701-1

Rangel CC, Carneiro LM, Bergqvist L, Oliveira EV, Goin FJ, Babot MJ (2019) Diversity, affinities and adaptations of the South American basal sparassodont *Patene* Simpson, 1935 (Mammalia, Metatheria). Ameghiniana 56: 263–289. https://doi.org/10.5710/AMGH.06.05.2019.3222

Rougier GW, Wible JR, Novacek MJ (1998) Implications of *Deltatheridium* specimens for early marsupial history. Nature 396: 459–463. https://doi.org/10.1038/24856

Savriama Y, Valtonen M, Kammonen JI, Rastas P, Smolander O-P, Lyyski A, Häkkinen TJ, Corfe IJ, Gerber S, Salazar-Ciudad I, Paulin L, Holm L, Löytynoja A, Auvinen P, Jernvall J (2018) Bracketing phenogenotypic limits of mammalian hybridization. Royal Society Open Science 5: 180903. http://dx.doi.org/10.1098/rsos.180903

Schultz JA, Menz U, Winkler DE, Schulz-Kornas E, Engels S, Kalthoff DC, Koenigswald WV, Ruf I, Kaiser TM, Kullmer O, Südekum K-H, Martin T (2018) Modular wear facet nomenclature for mammalian post-canine dentitions. Historical Biology 30: 30–41. https://doi.org/10.1080/08912963.2017.1302442

Simpson GG (1948) The beginning of the age of mammals in South America, Part 1. Bulletin of the American Museum of Natural History 91: 1–232.

Simpson GG (1971) The evolution of marsupials in South America. Anais da Academia Brasileira de Ciências 43: 103–118.

Smits PD, Evans AR (2012) Functional constraints on tooth morphology in carnivorous mammals. BMC Evolutionary Biology 12: 146. https://doi.org/doi:10.1186/1471-2148-12-146

Suárez C (2019) Estudios taxonómicos y paleobiológicos sobre los Metatheria (Mammalia) del Mioceno medio de La Venta, Colombia. PhD Thesis, Universidad Nacional de La Plata, Buenos Aires, Argentina, 560 pp. http://sedici.unlp.edu.ar/handle/10915/75246 [Accessed on 22.02.2022]

Taylor LA, Kaiser TM, Schwitzer C, Müller DW, Codron D, Clauss M, Schulz E (2013) Detecting inter-cusp and inter-tooth wear patterns in Rhinocerotids. PLoS One. 8:e80921. https://doi.org/10.1371/journal.pone.0080921

Teaford MF (2007) What do we know and not know about diet and enamel structure? In: Ungar PS (Ed) Evolution of the Human Diet: The Known, the Unknown, and the Unknowable. Oxford University Press, New York, 56–76.

Turnbull WD (1970) Mammalian masticatory apparatus. Fieldiana Geology 18: 149–356. http://hdl.handle.net/10111/UIUCOCA:mammalianmastica182turnb [Accessed on 22.02.2022]

Ungar PS (2005) Reproductive fitness and tooth wear: Milking as much as possible out of dental topographic analysis. Proceedings of the Academy of Science of the United Sates of America 102: 16533–16534. https://doi.org/10.1073/pnas.0508642102

Ungar PS (2010) Mammal teeth. Origin, Evolution, and Diversity. The Johns Hopkins University Press, Maryland, USA, 304 pp.

Ungar PS (2015) Mammalian dental function and wear: A review. Biosurface and Biotribology 1: 25–41. https://doi.org/10.1016/j.bsbt.2014.12.001

van Valkenburgh B (1988) Trophic diversity in past and present guilds of large predatory mammals. Paleobiology 14: 155–173. https://doi:10.1017/S0094837300011891

van Valkenburgh B (1989) Carnivore dental adaptations and diet: A study of trophic diversity within guilds. In: Gittleman JL (Ed) Carnivore Behaviour, Ecology, and Evolution. Cornell University Press, Ithaca, 410–436.

van Valkenburgh B (1990) Skeletal and dental predictors of body mass in carnivores. In: Damuth J, Macfadden BJ (Eds) Body Size in Mammalian Paleobiology. Estimation and Biological Implications. Cambridge University Press, Cambridge, 181–206.

van Valkenburgh B (1991) Iterative evolution of hypercarnivory in canids (Mammalia: Carnivora): Evolutionary interactions among sympatric predators. Paleobiology 17: 340–362. https://doi.org/10.1017/S0094837300010691

Vitek NS, Roseman CC, Bloch J (2020) Mammal molar size ratios and the inhibitory cascade at the intraspecific scale. Integrative Organismal Biology 2: obaa020, https://doi.org/10.1093/iob/obaa020

Werdelin L (1989) Constraint and adaptation in the bone-cracking canid *Osteoborus* (Mammalia: Canidae). Paleobiology 15: 387–401.

Zimicz AN (2012) Ecomorfología de los marsupiales paleógenos de América del Sur. PhD Thesis, Universidad Nacional de La Plata, Buenos Aires, Argentina. https://doi.org/10.35537/10915/29337

Zimicz N (2014) Avoiding competition: the ecological history of late Cenozoic metatherian carnivores in South America. Journal of Mammalian Evolution 21: 383–393. https://doi.org/10.1007/s10914-014-9255-8